Importance of the C-Terminal Helix to the Stability and Enzymatic Activity of *Escherichia coli* Ribonuclease H[†]

Eric R. Goedken, Tanya M. Raschke, and Susan Marqusee*

Department of Molecular and Cell Biology, University of California, Berkeley, 229 Stanley Hall, Berkeley, California 94720

Received January 10, 1997; Revised Manuscript Received March 10, 1997

ABSTRACT: The ribonuclease H (RNase H) family of enzymes selectively degrades the RNA strand of RNA·DNA hybrids. This activity is essential for retroviruses such as HIV and resides in a domain of the larger reverse transcriptase molecule. RNase H from *Escherichia coli* is the best-characterized member of the family and serves as a model for structure/function studies. Despite having almost identical $\alpha + \beta$ folds, the isolated domain from HIV is inactive and much less stable than the *E. coli* homolog. The HIV domain also shows increased disorder in its C-terminal regions (E-helix and His-containing loop). We investigated the importance of this region by studying a variant of *E. coli* RNase H lacking these elements (RNHΔE). Despite the elimination of 33 of 155 residues (including a complete helix), this C-terminal deletion mutant folds cooperatively as a subdomain. Surprisingly, this protein lacking residues near the active site retains weak Mn^{2+}-dependent activity. A peptide corresponding to the deleted E-helix is helical in isolation and stimulates the activity of the deletion mutant *in vitro*. These results have implications for the catalytic mechanism of RNase H and drug design targeted to HIV reverse transcriptase.

Ribonuclease H (RNase H)[1] is a divalent cation-dependent nuclease selective for the RNA strand of RNA·DNA hybrids. The RNases H comprise a large family of structurally-related enzymes from both prokaryotes and eukaryotes (Hostomsky et al., 1993). *Escherichia coli* RNase HI is the most thoroughly-characterized member of this family, although the biological role of this enzyme is not yet well-defined. In retroviruses, however, RNase H exists as a domain of the larger heterodimeric reverse transcriptase (RT) molecule. An active RNase H within HIV RT is essential for the conversion of the retroviral RNA genome into doubled-stranded DNA and is absolutely required for the production of infectious virions (Tisdale et al., 1991). As such, RNase H serves as an ideal drug target for anti-HIV therapy. Studies on the structure and function of this family of enzymes will provide an important foundation for the design of such inhibitors.

Functional studies of the RNase H family are aided by the existence of several high-resolution X-ray crystal structures including *E. coli* RNase HI (Katayanagi et al., 1990; Yang et al., 1990) and the isolated RNase H domain of reverse transcriptase from HIV-1 (Davies et al., 1991). All of these structures reveal a very similar $\alpha + \beta$ fold (Figure 1). However, while the *E. coli* protein is highly active *in vitro*, in either a Mg^{2+}- or Mn^{2+}-dependent manner, the isolated HIV domain is completely inactive with either metal. This is surprising given that the HIV domain is folded and contains all of the conserved residues believed to be necessary for RNase H activity. How then can we account for the difference in activity between the two homologs?

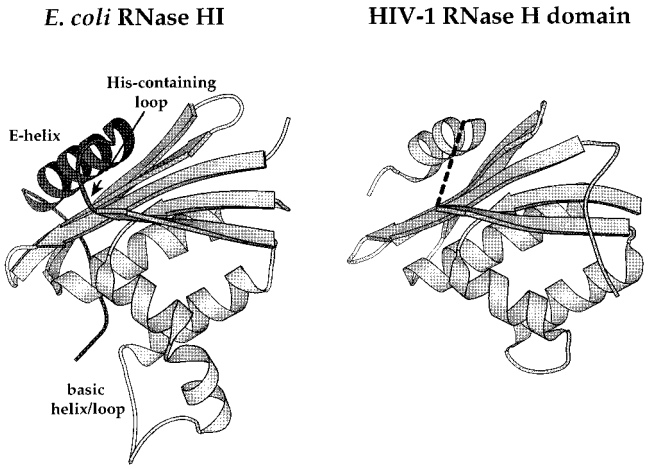

FIGURE 1: Comparison of the X-ray crystal structures of *E. coli* RNase H (Katayanagi et al., 1990; Yang et al., 1990) and the isolated HIV RNase H domain (Davies et al., 1991) [drawn with MOLSCRIPT (Kraulis, 1991)]. The C-terminal regions omitted in RNHΔE are darkened. The dashed line in the HIV RNase H structure represents the His-containing loop where no electron density was observed.

Several differences between the *E. coli* and HIV proteins could, in principle, explain this distinction in enzymatic activity (Figure 1). The most striking is the absence of the basic helix/loop region in the HIV enzyme. This basic helix/loop is believed to contribute to proper substrate binding and positioning in *E. coli* RNase H (Kanaya et al., 1991). A further distinction between these two homologs has been noted in their overall thermodynamic stability and flexibility, particularly at the C-terminus (Davies et al., 1991; Powers et al., 1991; Keck & Marqusee, 1996). These differences in the C-terminus may also explain the observed dichotomies in activity and stability between the two homologs.

[†] This work was supported by a grant from the NIH (GM53321).

* To whom correspondence should be addressed. Telephone: 510-642-7678. Fax: 510-643-9290. E-mail: marqusee@zebra.berkeley.edu.

[⊗] Abstract published in *Advance ACS Abstracts,* May,15, 1997.

[1] Abbreviations: CD, circular dichroism; C_m, midpoint concentration; DNA, deoxyribonucleic acid; *E. coli*, *Escherichia coli*; GdnHCl, guanidine hydrochloride; HIV, human immunodeficiency virus; RNA, ribonucleic acid; RNase H, ribonuclease H; RNase H*, fully active variant of *E. coli* ribonuclease H with three free cysteines replaced with alanine; RNHΔE, C-terminal deletion mutant of *E. coli* RNase H*; RT, reverse transcriptase; T_m, midpoint temperature.

S0006-2960(97)00060-3 CCC: $14.00

In the crystal structure of *E. coli* RNase H, the C-terminal region, namely, the E-helix and the loop connecting it to the rest of the protein, is ordered: the helix is securely packed against β-strands 1−3 (Katayanagi et al., 1990; Yang et al., 1990). In the HIV RNase H crystal structure, however, the corresponding loop is apparently disordered and shows no electron density (Davies et al., 1991). This loop is referred to as the "His-containing loop" because it contains a conserved histidine necessary for viral reproduction (Tisdale et al., 1991). NMR studies on the isolated HIV RNase H domain have also shown that in solution the E-helix is flexible and unstructured (Powers et al., 1991). Therefore, the ordering of this helix in the HIV RNase H crystal structure is likely due to crystal-packing interactions. However, in the context of the intact HIV reverse transcriptase containing an active RNase H moiety, this region is well-ordered (Kohlstaedt et al., 1992). Thus, the ordering and packing of the C-terminal E-helix seem to correlate with RNase H activity.

The C-terminal region of RNase H contains several residues that are considered important for its catalytic mechanism, including a conserved histidine within the loop (His 124 in *E. coli*) and a conserved aspartic acid within the E-helix (Asp 134 in *E. coli*). Mutations at either of these residues can dramatically reduce activity (Oda et al., 1993; Haruki et al., 1994b). Deletion of the last eight residues of *E. coli* RNase H (not including the E-helix) causes a moderate (40%) reduction in activity and a large loss in thermodynamic stability (∼4 kcal/mol) (Haruki et al., 1994a). Despite these mutational studies, the significance of the C-terminal region of RNase H remains unclear.

In this report, we address the importance of the C-terminal region through the analysis of a mutant *E. coli* protein, RNHΔE, which lacks the E-helix and adjacent residues (the C-terminal 33of 155 residues). By deleting these residues, we have essentially modeled the C-terminal disorder of the isolated HIV RNase H domain onto the framework of the *E. coli* protein. Despite the elimination of ∼20% of the sequence (including a large region of secondary structure) from a single-domain enzyme, the resulting protein, RNHΔE, folds cooperatively. Surprisingly, this mutant protein lacking the important His-containing loop and the E-helix retains weak Mn^{2+}-dependent activity. Furthermore, a synthetic peptide corresponding to the sequence of the deleted E-helix shows intrinsic helicity and, when combined with RNHΔE, is able to stimulate its activity *in vitro*. These studies lend insight into the catalytic mechanism of RNase H and should aid in the eventual design of targeted retroviral inhibitors.

MATERIALS AND METHODS

Expression and Purification of RNHΔE. A plasmid directing the expression of a C-terminal deletion mutant, RNHΔE (pTR102), was created by cassette mutagenesis of pSM101 (Dabora & Marqusee, 1994). Details of this plasmid are available upon request. *E. coli* BL21 (DE3) cells transformed with pLysS (Novagen) and pTR102 were grown at 37 °C in Luria-Bertani (LB) media with 200 μg of ampicillin/mL. Overexpression of RNHΔE was induced by adding isopropyl β-D-thiogalactopyranoside (1 mM) to cells at midlogarithmic phase (OD_{600} = ∼0.6). After 3 h additional growth, cells were harvested by centrifugation and stored at −80 °C until further processing.

Frozen cell pellets were resuspended in 10 mM Tris, pH 8.0, 0.1 mM EDTA, 20 mM NaCl and lysed by sonication on ice. Following centrifugation, the RNHΔE protein was found to remain in the insoluble portion, presumably in inclusion bodies. Pellets were resuspended in 50 mM Tris, pH 8.0, 1 mM EDTA and sonicated further on ice. Following a second centrifugation, the resulting pellet was washed thoroughly in 0.5% methionine and pelleted again by centrifugation. RNHΔE was extracted from this pellet by stirring overnight in 50% acetonitrile, 0.2% trifluoroacetic acid at room temperature. Insoluble material was removed by centrifugation.

RNHΔE in 50% acetonitrile, 0.2% TFA was diluted ∼4 fold with H_2O and purified over a Vydac C-18 reversed-phase HPLC column using a Shimadzu SCL-10A system controller. Resulting peak fractions were lyophilized and resuspended in H_2O. Purity was judged to be >95% by polyacrylamide gel electrophoresis stained with Coomassie brilliant blue. Electrospray-ionization mass spectrometry confirmed the expected molecular weight of RNHΔE within 1 Da. Protein concentrations were determined by UV absorbance spectroscopy at 280 nm in 6 M GdnHCl using a calculated extinction coefficient of 39 260 M^{-1} cm^{-1} based upon six tryptophans and four tyrosines (Edelhoch, 1967). RNHΔE used for activity studies was purified using the same method except expression was carried out in *E. coli* MIC1066 cells (kindly provided by Robert Crouch, NIH) which contain a T7 expression system and lack endogenous *E. coli* RNase H.

Synthesis and Purification of E-Helix Peptide. The E-helix peptide (sequence Ac-YGHPENERADELARAAA-NH_2) was synthesized on an ABI 431 peptide synthesizer using standard FMOC chemistry. Cleaved peptide was resuspended in 0.1% TFA, purified over a Vydac C-18 reversed-phase HPLC column, and lyophilized. The molecular weight of the resulting peptide was confirmed by electrospray-ionization mass spectrometry. Peptide was resuspended in H_2O, and concentrations were determined by UV absorbance spectroscopy at 280 nm in 6 M GdnHCl using a calculated extinction coefficient of 1280 M^{-1} cm^{-1} based upon a single tyrosine (Edelhoch, 1967).

RNase H Activity Assays. RNA·DNA hybrid was synthesized from M13K07 single-stranded DNA as described previously (Keck & Marqusee, 1995). RNase H reaction assays were conducted in standard buffer conditions of 50 mM Tris, pH 8.0, 50 mM NaCl, 1 μM (base pairs) RNA·DNA hybrid, 2.5% glycerol, 1.5 μM bovine serum albumin (BSA) unless otherwise specified; 1 μL of a saturated solution of linear polyacrylamide was added per 20 μL of reaction mixture to help maintain solubility of the substrate in the presence of divalent cation. Enzymes were diluted from concentrated stocks to final stock concentrations just prior to starting the reaction. Enzyme concentrations in the assays varied from 5 to 500 nM. Following specified incubation times at 37 °C, 20 μL reaction aliquots were stopped by the addition of 50 mM EDTA, 200 μg/mL *Torula* RNA (final concentration). The remaining uncleaved substrate was precipitated by adding 5% trichloroacetic acid and 20 mM sodium pyrophosphate (final concentrations). Following incubation on ice for 10 min, uncleaved substrate was pelleted in a microcentrifuge at maximum speed for 10 min. The acid-soluble radioactivity present in 90% of the supernatant was determined by liquid scintillation counting.

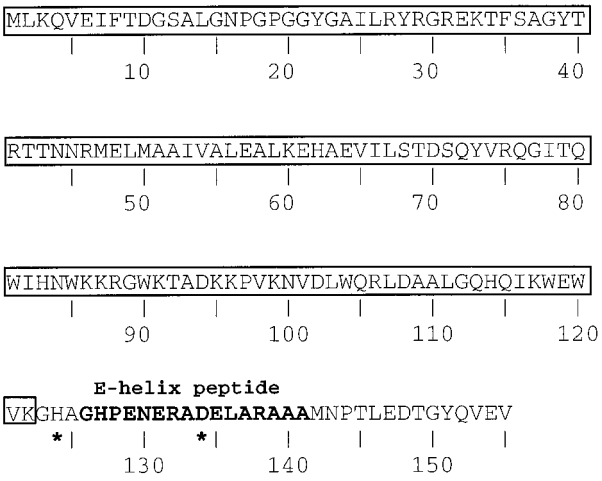

FIGURE 2: Amino acid sequence of RNase H*. The sequence of RNHΔE is boxed, and the E-helix peptide residues are in bold. Residues His 124 and Asp 134 are identified by asterisks.

Circular Dichroism Measurements. Circular dichroism (CD) data were collected using an Aviv 62DS spectropolarimeter with a Peltier temperature-controlled sample holder and 1 cm path length cuvette. Protein denaturation studies were conducted by monitoring the ellipticity at 222 nm as a function of temperature or GdnHCl concentration. Free energy of folding [assuming a two-state transition and linear dependence on denaturant (Santoro & Bolen, 1988)], midpoint denaturant concentrations (C_ms), and midpoint temperatures (T_ms) were calculated as described by Dabora and Marqusee (1994) using the nonlinear least-squares fitting program NONLIN (Johnson & Fraisier, 1985).

Full length RNase H* used for activity assays and circular dichroism studies was a gift from Aaron Chamberlain (Chamberlain et al., 1996). [RNase H* is a fully active variant of *E. coli* RNase H in which the three free cysteines have been replaced with alanine (Kanaya et al., 1990; Dabora & Marqusee, 1994)]. HIV RNase H (consisting of residues 427−560 of HIV-1 reverse transcriptase plus an initiator methionine) used in thermal denaturation studies was a gift from Gunther Kern. This protein was induced from the overexpression construct pCC101 as described in Keck and Marqusee (1995).

RESULTS

Construction of a C-Terminal Deletion Mutant, RNHΔE. A plasmid vector (pTR102) carrying the gene sequence of the C-terminal deletion mutant of *E. coli* RNase H* was created by cassette mutagenesis of pSM101. [RNase H* is a cysteine-free variant of *E. coli* RNase H which displays comparable activity to the wild type (Kanaya et al., 1990; Dabora & Marqusee, 1994).] A stop codon was introduced after Lys 122 (Figure 2) which is immediately C-terminal to the last residue within β-strand 5. The resulting protein sequence (RNHΔE) omits the 33 terminal residues (Gly 123−Val 155) which include the E-helix and its preceding loop. The coding region of pTR102 was confirmed by DNA sequencing, and the purified RNHΔE protein was found to have the expected molecular weight within 1 Da by mass spectrometry (data not shown).

C-Terminal Deletion Mutant RNHΔE Is Folded. The far-UV CD spectrum of RNHΔE was indicative of a well-folded highly helical protein (Figure 3a). The parent protein, full length RNase H*, displayed a mixed $\alpha + \beta$ CD spectrum consistent with the wild type *E. coli* RNase H crystal structure (Katayanagi et al., 1990; Yang et al., 1990). In comparison to RNase H*, the spectrum of RNHΔE is suggestive of a higher relative helix content with characteristic minima at 222 and 208 nm and greater mean residue ellipticity below 230 nm. This result was unexpected given the removal of a complete helix (the E-helix) from the parent protein. The increase in helical signal may be the result of structural alterations (increased disorder) in the β-sheet region of the protein in response to the elimination of the interacting, proximal C-terminal residues.

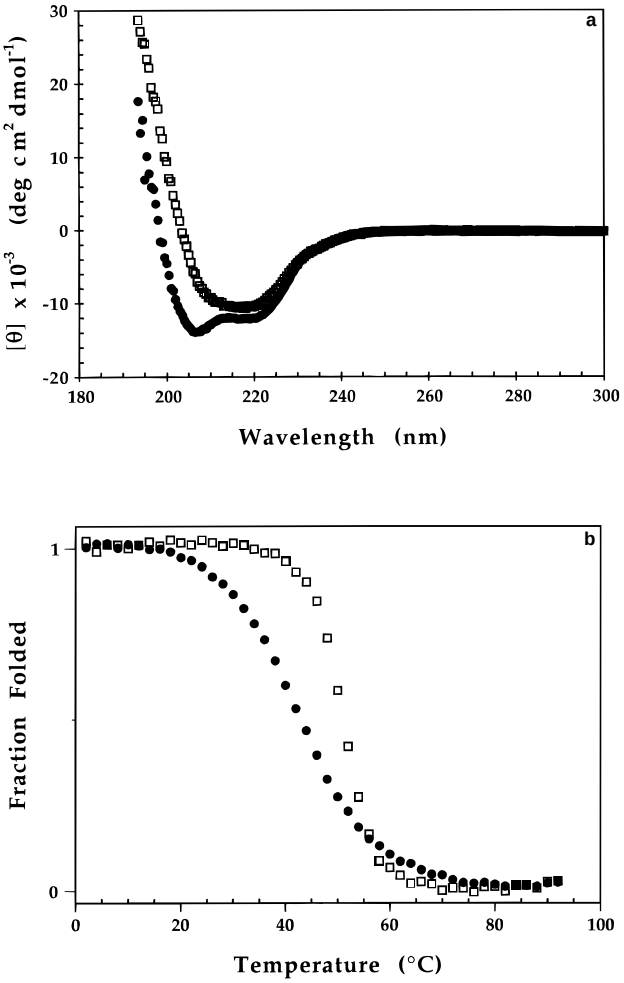

FIGURE 3: Circular dichroism spectra and thermal denaturation of *E. coli* RNase H* and RNHΔE. (a) Far-UV circular dichroism spectra of RNase H* (□) and RNHΔE (●). The spectra were collected using a 1 cm path length cuvette at 25 °C in 5 mM potassium fluoride, 2 mM potassium phosphate, pH 8.0 with 50 μg/mL protein. (b) Thermal denaturation curves of RNase H* (□) and RNHΔE (●). Data were collected by monitoring the circular dichroism signal at 222 nm and converting to fraction folded as described in Dabora and Marqusee (1994). (20 mM potassium chloride, 100 mM potassium phosphate, pH 8.0, 0.8 M guanidine hydrochloride). Melts were >90% reversible as measured by the recovery of signal at 2 °C.

The CD signal at 222 nm was linearly dependent on RNHΔE concentration from 0 to 75 μg/mL in 100 mM potassium phosphate, 20 mM potassium chloride, pH 8.0 (data not shown). This suggests that the folded protein fragment is monomeric under these conditions.

*RNHΔE Unfolds Cooperatively but Is Less Stable than RNase H**. Thermal denaturation of RNHΔE monitored by

Table 1: Thermodynamic Stability of *E. coli* RNase H*, RNHΔE, and the Isolated RNase H Domain from HIV RT[a]

protein	T_m(0.8 M GdnHCl), °C	C_m(GdnHCl), M	$\Delta G_{fold}(H_2O)$, kcal/mol
E. coli RNase H*	50.9	1.6[b]	−7.2[b]
RNHΔE	42.5	1.3	−3.0
HIV RNase H domain	45.6	1.2[c]	−4.0[c]

[a] Values were determined by reversible thermal denaturation or reversible GdnHCl denaturation at pH 8.0 as monitored by the circular dichroism signal at 222 nm. [b] From Dabora and Marqusee (1994). [c] From Keck and Marqusee (1995).

following the CD signal at 222 nm showed cooperative unfolding with a midpoint temperature (T_m) of 42.5 °C in 0.8 M guanidine hydrochloride (GdnHCl) (Figure 3b). GdnHCl was included in these experiments to prevent aggregation at high temperature and to assure >90% reversibility. The full length parent protein, RNase H*, unfolded even more cooperatively with a T_m of 50.9 °C (Figure 3b).

GdnHCl-induced denaturation of RNHΔE was also cooperative. The extrapolated free energy of unfolding, $\Delta G_{unf}(H_2O)$, was 3.0 kcal/mol (C_m=1.3 M), assuming a two-state transition (Santoro & Bolen, 1988). Table 1 shows a comparison of these stability data for RNHΔE and its homologs. By all criteria, the deletion mutant is less stable than RNase H*. Thus, the elimination of the E-helix region causes a significant loss in stability but does not cripple the mutant's overall ability to fold. The cooperative unfolding of RNHΔE by both heat and chemical denaturant suggests that the protein is forming a well-folded, compact native state and not a poorly-folded, molten globule-like species. Hence, RNHΔE appears to form a folded subdomain of the single-domain parent protein, *E. coli* RNase H*.

RNHΔE Retains Mn^{2+}-Dependent Activity. In order to address the specificity of the tertiary fold of RNHΔE, we assayed the fragment for RNase H activity. Enzymatic activity was monitored by following the release of acid-soluble radiolabeled RNA·DNA substrate. In the presence of Mg^{2+} (Figure 4a), no activity was observed with 250 nM RNHΔE. Under the same conditions, 5 nM full length RNase H* rapidly catalyzed the release of most of the substrate. In 1 mM $MnCl_2$ at 37 °C, however, 250 nM RNHΔE showed detectable activity (Figure 4b), although it was approximately 100-fold less effective in cleaving RNA·DNA hybrid than RNase H* under the same conditions. This comparison may not be completely valid, though, since recent work has shown that high levels of Mn^{2+} (>5 μM) will inhibit the activity of either RNase H* or wild type *E. coli* RNase H (Keck & Marqusee, 1996, 1997). Nonetheless, RNHΔE clearly shows Mn^{2+}-dependent activity suggesting it retains a structure similar to that of the wild type.

To further examine the Mn^{2+} dependence of our C-terminal deletion mutant, we titrated 200 nM RNHΔE with varying amounts of $MnCl_2$ and followed the resulting activity (Figure 5). Detectable activity began around 0.5 mM $MnCl_2$ and increased rapidly above 2 mM. Maximum activity was seen near 10 mM $MnCl_2$. (Some precipitation was observed in samples at and above 50 mM $MnCl_2$, presumably due to the reaction of Mn^{2+} with the buffering components.) No activity was observed in $MgCl_2$ (500 nM RNHΔE, 0−10 mM $MgCl_2$, data not shown).

To determine whether the inhibition observed at the higher $MnCl_2$ concentrations resulted from nonspecific changes in the ionic strength of the assay conditions, we monitored activity as a function of NaCl in 3 mM $MnCl_2$ (Figure 6). Addition of NaCl resulted in the inhibition of activity at comparable ionic strengths to that observed in the $MnCl_2$ titration. By 150 mM NaCl, activity was virtually eliminated, which paralleled the effect of 50 mM $MnCl_2$. Results showing very similar inhibition were obtained using KF (data not shown). Hence, the inhibition of activity seen for RNHΔE at high Mn^{2+} concentrations may result from a general effect of ionic strength. The inhibition seen at low Mn^{2+} concentrations (>5 μM) for full length *E. coli* RNase

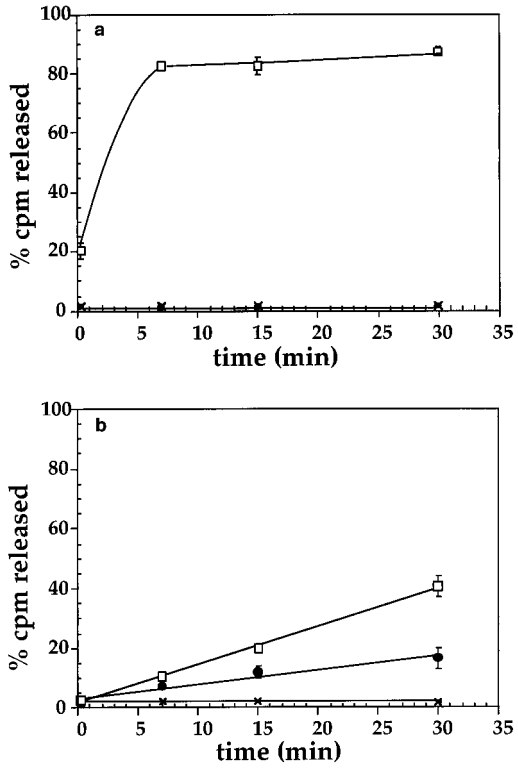

FIGURE 4: RNase H activity assays of RNase H* and RNHΔE. Reactions were conducted at 37 °C in 1 mM divalent cation ($MgCl_2$ or $MnCl_2$), 50 mM Tris, pH 8.0, 50 mM NaCl, 1 μM (base pairs) RNA·DNA hybrid, 2.5% glycerol, 0.1 mg/mL linear polyacrylamide, 1.5 μM BSA for the times indicated. The percentage of acid-soluble substrate released was determined by liquid scintillation counting. Error bars represent the standard deviation of at least two separate reactions, and those that are not visible are smaller than the size of the symbol. (a) Mg^{2+}-dependent activity of 5 nM RNase H* (□), 250 nM RNHΔE (●), and no enzyme control (×). (b) Mn^{2+}-dependent activity of 5 nM RNase H* (□), 250 nM RNHΔE (●), and no enzyme control (×).

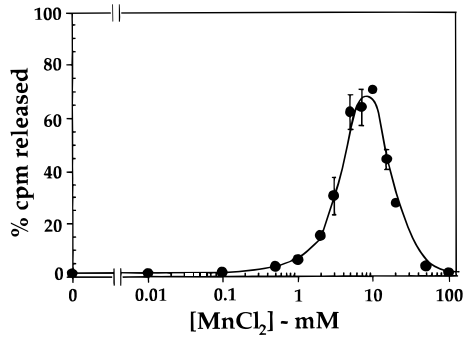

FIGURE 5: Activity of 200 nM RNHΔE as a function of $MnCl_2$ concentration. Buffer conditions were otherwise the same as in Figure 4. Reactions were stopped after 15 min incubation at 37 °C. Error bars are as described in Figure 4.

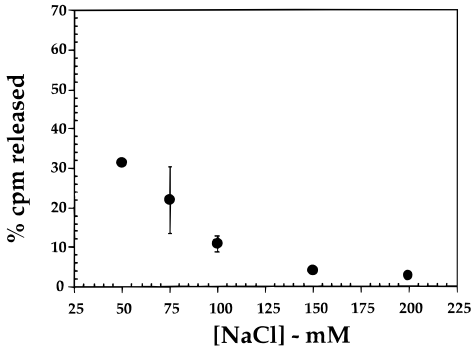

FIGURE 6: Activity of 200 nM RNHΔE in 3 mM $MnCl_2$ as a function of NaCl concentration. Buffer conditions were otherwise the same as in Figure 4. Reactions were stopped after 15 min incubation at 37 °C. Error bars are as described in Figure 4.

H, however, appears to be a specific Mn^{2+} effect (Keck & Marqusee, 1996, 1997).

A Peptide from the E-Helix Folds in Isolation. To further investigate the structure/function relationship of the C-terminus of RNase H*, we synthesized a peptide (sequence Ac-YGHPENERADELARAAA-NH_2) consisting of the 16 residues from the E-helix plus an N-terminal tyrosine to allow quantitation of the peptide by UV spectroscopy (Figure 2). Far-UV CD spectroscopy showed that this peptide folds into an α-helix independently of the rest of the protein (Figure 7a). The E-helix peptide is roughly 40% helical under these conditions [assuming a signal at 222 nm of −32 000 deg·cm^2/dmol corresponds to 100% helix and a value of 0 for the random coil (Marqusee et al., 1989)]. The helical peptide is apparently monomeric as the concentration dependence of the CD signal at 222 nm was linear between 0 and 100 μM (data not shown). The E-helix peptide showed a broad thermal denaturation (Figure 7b) as expected for a small peptide helix. Thus, residues 126−141 of RNase H* have a high intrinsic helical propensity. Such high helical content is unusual for such small peptides.

The E-Helix Peptide Stimulates the Mn^{2+}-Dependent Activity of RNHΔE. Given that the E-helix peptide is helical and carries the equivalent of the catalytically-important Asp 134, we studied the effect of adding the peptide to RNHΔE. Addition of the E-helix peptide did not alter activity in 1 mM $MgCl_2$ where no release of substrate was observed in the presence of 250 nM RNHΔE + 50 μM E-helix (data not shown). However, the E-helix peptide showed a dramatic effect on Mn^{2+}-dependent activity when combined in 200-fold excess with RNHΔE. In 1 mM $MnCl_2$, activity was substantially increased relative to RNHΔE alone (Figure 8a). Presumably this stimulation is the result of a specific interaction between RNHΔE and the E-helix peptide: the E-helix peptide alone demonstrated no activity (Figure 8a), and a peptide from the same region of HIV RNase H (sequence Ac-YGGNEQVDKLVS-NH_2) at comparable concentrations did not alter RNHΔE activity (data not shown). Apparently, the E-helix peptide binds to RNHΔE in an orientation similar to that of the E-helix in the RNase H crystal structure and is thus able to increase the activity of RNHΔE.

By utilizing activity as a probe for the binding of the E-helix peptide to RNHΔE, we were able to estimate the dissociation constant (K_d) for this interaction. A titration of RNHΔE with the peptide showed increasing activity as a function of peptide concentration (Figure 8b). At 40 nM

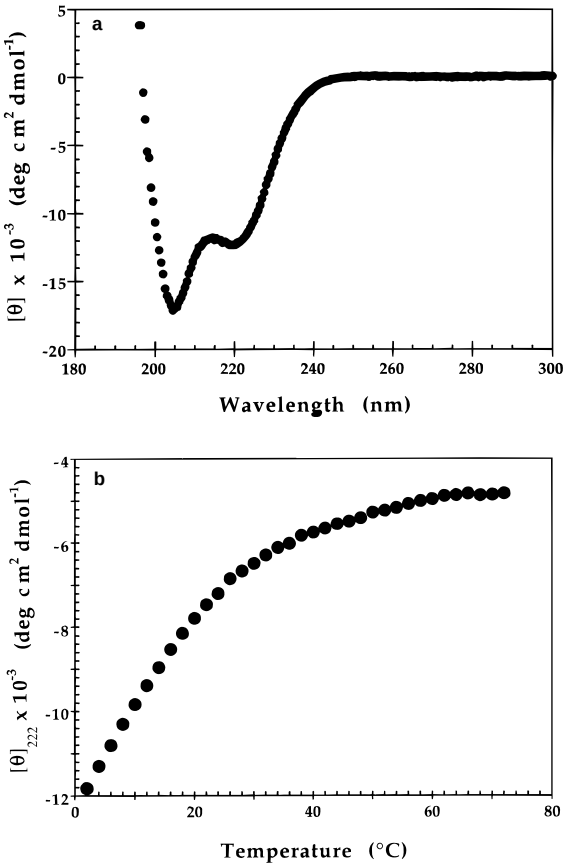

FIGURE 7: Circular dichroism spectrum and thermal denaturation of the E-helix peptide. (a) Far-UV circular dichroism spectrum of the E-helix peptide. The spectrum was collected using a 1 cm path length cuvette at 2 °C in 5 mM potassium fluoride, 2 mM potassium phosphate, pH 8.0, with 50 μg/mL peptide. (b) Thermal denaturation curve of the E-helix peptide. Data were collected by monitoring the circular dichroism signal at 222 nm. Buffer conditions were 20 mM potassium chloride, 100 mM potassium phosphate, pH 8.0.

RNHΔE, where no detectable activity was observed in standard assay conditions [1 μM (bp) RNA·DNA hybrid, 1 mM $MnCl_2$, 37 °C], addition of 200 μM peptide stimulated RNase H activity such that over 60% of the substrate was released in 15 min. This experiment suggests a dissociation constant for the peptide and RNHΔE on the order of 50 μM at 37 °C. This estimation does not include the contribution of the helix−coil equilibrium of the peptide and therefore underestimates the actual affinity of the peptide in its helical conformation for RNHΔE.

DISCUSSION

E. coli RNase H serves as a model for the structure and function of a large family of homologous enzymes that degrade the RNA strand of DNA·RNA hybrids. Because the RNase H activity within reverse transcriptase is essential for retroviral reproduction, a biochemical understanding of the structure and function of this enzyme is important for the design of targeted drug inhibitors to HIV. These studies are aided by the high-resolution X-ray crystal structures for both the *E. coli* protein (Katayanagi et al., 1990; Yang et al., 1990) and the isolated domain from the HIV-1 reverse transcriptase heterodimer (Davies et al., 1991). Despite having a very similar α + β fold (Figure 1), the isolated domain from HIV is inactive.

The observed inactivity in the isolated HIV domain is particularly puzzling because it contains all of the conserved

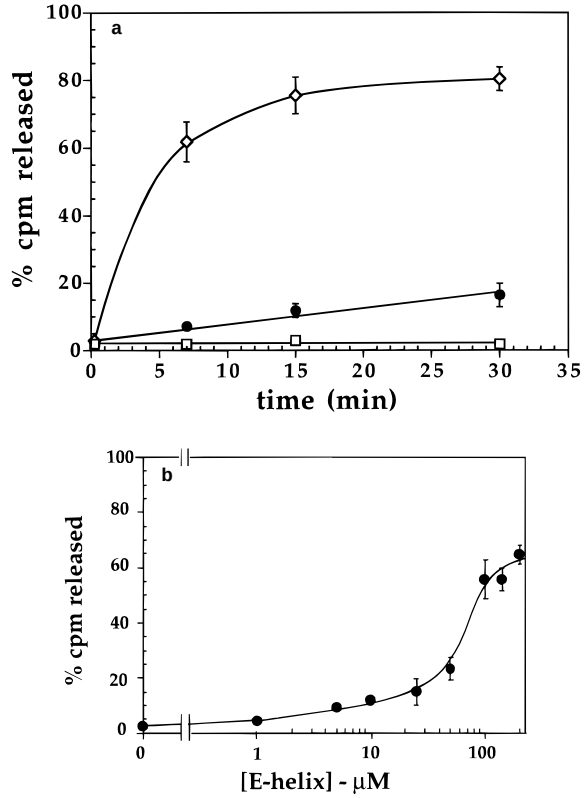

FIGURE 8: E-Helix peptide stimulates Mn^{2+}-dependent activity of RNHΔE. (a) Activity of 250 nM RNHΔE (●), 250 nM RNHΔE + 50 μM E-helix peptide (◇), and 50 μM E-helix (□) in 1 mM $MnCl_2$. Buffer conditions and error bars are as described in Figure 4. (b) Activity of 40 nM RNHΔE as a function of E-helix peptide concentration in 1 mM $MnCl_2$. Reactions were stopped after 15 min incubation at 37 °C. Buffer conditions and error bars are as described in Figure 4.

residues considered critical for catalysis in the *E. coli* homolog. An obvious difference between the two, however, is the absence of the basic helix/loop in the HIV domain, and the role of this region has been explored in several studies. Because mutations in this region of the *E. coli* protein result in enzymes with increased Michaelis constants (K_ms), it was initially suggested that this basic region is crucial for proper substrate binding and positioning (Kanaya et al., 1991). In the context of reverse transcriptase, the polymerase domain may serve in this role. Indeed, substitution of the *E. coli* basic helix/loop into HIV RNase H restores Mn^{2+}-dependent activity and increases thermodynamic stability (Stahl et al., 1994; Keck & Marqusee, 1995). However, subsequent experiments have revealed that the elimination of the same region from *E. coli* RNase H does not abolish Mn^{2+}-dependent activity (Keck & Marqusee, 1996). In addition, the HIV RNase H domain has been shown to interact with substrate by fluorescence spectroscopy (Cirino et al., 1993). Therefore, it is now clear that while the basic helix/loop does contribute greatly to substrate recognition, its absence cannot completely account for the inactivity of the isolated HIV RNase H.

These two homologous proteins also differ in their thermodynamic stability and flexibility. The free energy of folding of *E. coli* RNase H is nearly 2 times that for the HIV protein (Keck & Marqusee, 1996), despite a similar structural architecture. Moreover, both NMR and X-ray crystallography have demonstrated that the C-terminal region (the E-helix region) of the HIV domain is dynamically disordered (Davies et al., 1991; Powers et al., 1991). Given that the packing and stability of the E-helix correlate with RNase H activity, we sought to model the C-terminal instability of the isolated HIV domain onto the *E. coli* enzyme by the deletion of the comparable C-terminal regions.

Stability of a Subdomain. Despite the elimination of a significant portion of secondary structure from the C-terminus, the deletion mutant RNHΔE folds cooperatively and is capable of RNase H activity. It is widely believed that the smallest cooperatively folding unit of a protein is a single domain (Kim & Baldwin, 1982; Creighton, 1993); indeed, many proteins lose the capacity to fold with the elimination of a small number of residues (Creighton, 1993). RNHΔE, however, is folded and retains moderate stability despite the loss of 33 amino acids. The role of this subdomain in the folding and stability of full length RNase H remains unclear. However, it is likely to be relevant to the folding pathway and partially-folded intermediates of RNase H which are currently under scrutiny in our laboratory (Chamberlain et al., 1996; Dabora et al., 1996; Raschke and Marqusee, 1997).

The subdomain's properties aid in our understanding of the relationship between stability and activity in the RNase H family. Keck and Marqusee (1996) have suggested that the partial activity of various RNase H mutants may be linked to their diminished stability. The free energy of unfolding of the inactive HIV RNase H is ∼4 kcal/mol at 25 °C compared to ∼7 kcal/mol for the highly active *E. coli* RNase H (Keck & Marqusee, 1996). The free energy of unfolding of partially active RNase H mutants has been shown to be intermediate (∼5−6 kcal/mol) (Keck & Marqusee, 1995, 1996). Mn^{2+} activation of catalysis in these partially active enzymes requires higher divalent cation concentrations (0.1−1 mM) than those required for wild type *E. coli* RNase H (∼2−5 μM) (Keck & Marqusee, 1997). Hence, reduced metal-binding affinity is evident in these less stable mutants. This correlation of affinity with overall stability may stem from a more precise active site arrangement in a rigidly-ordered, highly stable enzyme.

We found that deletion of the C-terminal 33 amino acids from *E. coli* RNase H results in a ∼4 kcal/mol reduction in stability (Table 1) and a loss in metal affinity (Figure 5). Deleting the basic helix/loop from the *E. coli* protein also results in a loss in stability (∼1.5 kcal/mol) (Keck & Marqusee, 1996). Therefore, the lack of the basic helix/loop and the disorder at the C-terminus in HIV RNase H destabilize the isolated domain. The reduced stability of HIV RNase H is likely related to its lack of activity when separated from reverse transcriptase. Within RT, domain−domain interactions may provide additional stability to the RNase H domain (Kohlstaedt et al., 1992). While RNHΔE has a reduced stability similar to the inactive HIV protein, it retains weak RNase H activity. This difference may be due to the additional substrate recognition conferred by the basic helix/loop which is present in RNHΔE but not in HIV RNase H.

Implications for RNase H Cation Dependent Mechanism. Deletion of the C-terminal 33 residues from *E. coli* RNase H* eliminates Mg^{2+}-dependent, but not Mn^{2+}-dependent activity (Figure 4). The activity of RNHΔE in 1 mM $MnCl_2$ is only ∼100-fold less than that observed for the full length protein in the same conditions but ∼10 000-fold less than that observed for the full length protein in 1 mM $MgCl_2$.

Thus, the C-terminal deletion causes the enzyme to undergo a switch in divalent cation preference at 1 mM concentrations from Mg^{2+} to Mn^{2+}. Other mutational studies in the RNase H family have also resulted in enzymes with activities dependent on Mn^{2+} but inactive with Mg^{2+}. These include a histidine-tagged HIV RNase H (Smith & Roth, 1993), the HIV basic helix/loop chimera (Stahl et al., 1994; Keck & Marqusee, 1995), and the basic helix/loop deletion from *E. coli* RNase H (Keck & Marqusee, 1996). This proclivity for Mn^{2+} dependence is particularly interesting given that the model protein *E. coli* RNase H shows greater activity with Mg^{2+} under most conditions.

RNHΔE is both activated and subsequently inhibited by $MnCl_2$. This inhibition can be explained by a nonspecific, electrostatic effect from the $MnCl_2$ because it can be mimicked by the addition of NaCl or KF. This is not surprising given that RNase H is a nonspecific ribonuclease, and much of its substrate recognition is thought to be due to electrostatic interactions provided by the basic helix/loop. Inhibition of activity by divalent cations has been seen in other RNases H at high concentrations, as well as by high amounts of NaCl (Black & Cowan, 1994; Keck & Marqusee, 1995). These observations can also be understood as resulting from electrostatic shielding.

The deleted regions in RNHΔE, namely, the E-helix and His-containing loop, contain side chains with functional groups which are important for ribonuclease H activity. How, then, is the RNHΔE fragment able to maintain activity without these important residues? Although His 124 is not absolutely required, its substitution reduces RNase H activity ~100-fold (Oda et al., 1993). E-Helix residue Asp 134 is also considered important for liganding a divalent cation in a proposed two-metal RNase H mechanism (Davies et al., 1991). In the alternatively-proposed single-metal RNase H mechanism (Oda et al., 1993), however, less emphasis is placed upon Asp 134. Nonconservative mutations of Asp 134 decrease activity ~1000-fold, and proponents of the single-metal mechanism suggest Asp 134 serves to help maintain a proper active site conformation rather than acts as a required second metal-binding site (Haruki et al., 1994b). Recent studies on the metal dependence (both Mn^{2+} and Mg^{2+}) of RNase H suggest that the enzyme probably functions through a single-metal mechanism which can be attenuated by the binding of a second metal (Keck & Marqusee, 1997). This model is simply a variation of the one-metal mechanism where the side chains of His 124 and Asp 134 provide a second inhibitory metal-binding site which attenuates the catalysis made possible by the binding of the first metal.

In this newly-proposed reaction mechanism His 124 and Asp 134 are less critical for activity. His 124 (which is deleted in RNHΔE) is proposed to be utilized for efficient deprotonatation of the catalytic residue Asp 70 after it abstracts a proton from the attacking nucleophilic water molecule. The 100-fold loss in activity seen in the substitution of His 124 to Ala (Oda et al., 1993) can then be explained by the cost of forcing Asp 70 to deprotonate by other means. While the deleted residues in RNHΔE, Asp 134 and His 124, are important to the maintenance of active site geometry and efficient catalysis in RNase H, they are not absolutely required, unlike the catalytic triad of Asp 10, Glu 48, and Asp 70.

The activity we observed in RNHΔE supports the activation/attenuation mechanism of RNase H catalysis. In the weakly active RNHΔE, neither His 124 nor Asp 134 are present. Thus, those residues are not absolutely required for ribonuclease H activity as predicted by the activation/attenuation model. Unless RNHΔE utilizes a completely different method of catalysis, these data are inconsistent with the two-metal mechanism. Even in the more active reconstituted RNase H (with the addition of the E-helix peptide), no equivalent of His 124 is present. This result combined with prior mutagenesis of this position (Oda et al., 1993) reaffirms the nonessential nature of this histidine. Thus, our findings help to corroborate our current model of the RNase H catalytic mechanism.

Implications of E-Helix Peptide Binding. The complementation of the RNase H fragment and the E-helix peptide is reminiscent of the classic bimolecular reconstitution of active ribonuclease A by the combination *in vitro* of inactive S-protein (residues 21−124) with S-peptide (residues 1−20) (Richards & Vithayathil, 1959). The large activation we observe in RNase H activity with RNHΔE (Figure 8) indicates that the subdomain maintains a specific affinity for the E-helix peptide. The intrinsic helicity of the E-helix peptide (Figure 7) is probably important to the moderate strength of this interaction ($K_d \approx 50\ \mu M$). Whether the chemical basis for this complementation is at the level of catalysis or thermodynamic stability is unclear. Mutagenesis of the E-helix peptide in combination with RNHΔE may provide further insight into the relationship between the E-helix and RNase H activity.

Regardless of the specific mechanism of activation by the E-helix peptide, the stability and ordering it provides to the active site seem to be important for its catalysis. These results suggest a likely explanation for the inactivity of the HIV domain: the disorder in the His-containing loop and the E-helix resulting from the removal of HIV RNase H from the RT heterodimer eliminates activity. This idea is supported by the observation that deletions of the HIV E-helix from RNase H in reverse transcriptase result in abolished viral infectivity (Tisdale et al., 1991). Considering that simply isolating the RNase H domain from the RT complex results in substantial entropy in the C-terminus, the interactions between the E-helix and the rest of RNase H appear relatively weak and, therefore, susceptible to inhibition by drug design. One could attempt to disrupt this already-compromised association and thereby inhibit activity by preventing complete folding of the RT heterodimer. A molecule that could preferentially bind to either the E-helix or the β-strands should substantially reduce RNase H activity and, in turn, infectious virions. Thus, the interface between the E-helix and the rest of RNase H is likely a good target for drug discovery against HIV.

ACKNOWLEDGMENT

We thank Jim Keck for critical reading of this manuscript and assistance with activity assays, David King for peptide synthesis and mass spectrometry, and all members of the Marqusee Laboratory for scientific advice and encouragement.

REFERENCES

Black, C. B., & Cowan, J. A. (1994) *Inorg. Chem. 33,* 5805−5808.

Chamberlain, A. K., Handel, T. M., & Marqusee, S. (1996) *Nature Struct. Biol. 3*, 782−786.
Cirino, N. M., Kalayjian, R. C., Jentoft, J. E., & LeGrice, S. F. (1993) *J. Biol. Chem. 268*, 14743−14749.
Creighton, T. (1993) *Proteins: Structures and Molecular Properties*, W. H. Freeman and Co., New York.
Dabora, J. M., & Marqusee, S. (1994) *Protein Sci. 3*, 1401−1408.
Dabora, J. M., Pelton, J. G., & Marqusee, S. (1996) *Biochemistry 35*, 11951−11958.
Davies, J. F., Hostomska, Z., Hostomsky, Z., Jordan, S. R., & Matthews, D. A. (1991) *Science 252*, 88−95.
Edelhoch, H. (1967) *Biochemistry 6*, 1948−1954.
Haruki, M., Noguchi, E., Akasako, A., Oobatake, M., Itaya, M., & Kanaya, S. (1994a) *J. Biol. Chem. 269*, 26904−26911.
Haruki, M., Noguchi, E., Nakai, C., Liu, Y. Y., Oobatake, M., Itaya, M., & Kanaya, S. (1994b) *Eur. J. Biochem. 220*, 623−631.
Hostomsky, Z., Hostomska, Z., & Matthews, D. A. (1993) *Ribonucleases H*, Cold Spring Harbor Laboratory Press, Plainview, NY.
Johnson, M. L., & Fraisier, S. G. (1985) *Methods Enzymol. 117*, 301−342.
Kanaya, S., Kimura, S., Katsuda, C., & Ikehara, M. (1990) *Biochem J. 271*, 59−66.
Kanaya, S., Katsuda, N. C., & Ikehara, M. (1991) *J. Biol. Chem. 266*, 11621−11627.
Katayanagi, K., Miyagawa, M., Matsushima, M., Ishikawa, M., Kanaya, S., Ikehara, M., Matsuzaki, T., & Morikawa, K. (1990) *Nature 347*, 306−309.
Keck, J. L., & Marqusee, S. (1995) *Proc. Natl. Acad. Sci. U.S.A. 92*, 2740−2744.
Keck, J. L., & Marqusee, S. (1996) *J. Biol. Chem. 271*, 19883−19887.
Keck, J. L., & Marqusee, S. (1997) *Tech. Protein Chem.* (in press).
Kim, P. S., & Baldwin, R. L. (1982) *Annu. Rev. Biochem. 51*, 459−489.
Kohlstaedt, L. A., Wang, J., Friedman, J. M., Rice, P. A., & Steitz, T. A. (1992) *Science 256*, 1783−1790.
Kraulis, P. J. (1991) *J. Appl. Crystallogr. 24*, 946−950.
Marqusee, S., Robbins, V. H., & Baldwin, R. L. (1989) *Proc. Natl. Acad. Sci. U.S.A. 86*, 5286−5290.
Oda, Y., Yoshida, M., & Kanaya, S. (1993) *J. Biol. Chem. 268*, 88−92.
Powers, R., Clore, G. M., Bax, A., Garrett, D. S., Stahl, S. J., Wingfield, P. T., & Gronenborn, A. M. (1991) *J. Mol. Biol. 221*, 1081−1090.
Raschke, T. M., & Marqusee, S. (1997) *Nature Struct. Biol. 4*, 298−304.
Richards, F. M., & Vithayathil, P. J. (1959) *J. Biol. Chem. 234*, 1459−1465.
Santoro, M. M., & Bolen, D. W. (1988) *Biochemistry 27*, 8063−8068.
Smith, J. S., & Roth, M. J. (1993) *J. Biol. Chem. 67*, 4037−4049.
Stahl, S. J., Kaufman, J. D., Vikic, T. S., Crouch, R. J., & Wingfield, P. T. (1994) *Protein Eng. 7*, 1103−1108.
Tisdale, M., Schulze, T., Larder, B. A., & Moelling, K. (1991) *J. Gen. Virol.* 59−66.
Yang, W., Hendrickson, W. A., Crouch, R. J., & Satow, Y. (1990) *Science 249*, 1398−1405.

BI970060Q